ARTICLE

Associations between [^{18}F]AV1451 tau PET and CSF measures of tau pathology in a clinical sample

Renaud La Joie, PhD, Alexandre Bejanin, PhD, Anne M. Fagan, PhD, Nagehan Ayakta, BS, Suzanne L. Baker, PhD, Viktoriya Bourakova, BS, Adam L. Boxer, MD, PhD, Jungho Cha, PhD, Anna Karydas, BS, Gina Jerome, MS, Anne Maass, PhD, Ashley Mensing, BS, Zachary A. Miller, MD, James P. O'Neil, PhD, Julie Pham, BA, Howard J. Rosen, MD, Richard Tsai, MD, Adrienne V. Visani, BS, Bruce L. Miller, MD, William J. Jagust, MD, and Gil D. Rabinovici, MD

Correspondence
Dr. La Joie
Renaud.Lajoie@ucsf.edu

Neurology® 2018;90:e282-e290. doi:10.1212/WNL.0000000000004860

Abstract

Objective
To assess the relationships between fluid and imaging biomarkers of tau pathology and compare their diagnostic utility in a clinically heterogeneous sample.

Methods
Fifty-three patients (28 with clinical Alzheimer disease [AD] and 25 with non-AD clinical neurodegenerative diagnoses) underwent β-amyloid (Aβ) and tau ([^{18}F]AV1451) PET and lumbar puncture. CSF biomarkers ($A\beta_{42}$, total tau [t-tau], and phosphorylated tau [p-tau]) were measured by multianalyte immunoassay (AlzBio3). Receiver operator characteristic analyses were performed to compare discrimination of Aβ-positive AD from non-AD conditions across biomarkers. Correlations between CSF biomarkers and PET standardized uptake value ratios (SUVR) were assessed using skipped Pearson correlation coefficients. Voxelwise analyses were run to assess regional CSF–PET associations.

Results
[^{18}F]AV1451-PET cortical SUVR and p-tau showed excellent discrimination between Aβ-positive AD and non-AD conditions (area under the curve 0.92–0.94; ≤0.83 for other CSF measures), and reached 83% classification agreement. In the full sample, cortical [^{18}F]AV1451 was associated with all CSF biomarkers, most strongly with p-tau ($r = 0.75$ vs 0.57 for t-tau and −0.49 for $A\beta_{42}$). When restricted to Aβ-positive patients with AD, [^{18}F]AV1451 SUVR correlated modestly with p-tau and t-tau (both $r = 0.46$) but not $A\beta_{42}$ ($r = 0.02$). On voxelwise analysis, [^{18}F]AV1451 correlated with CSF p-tau in temporoparietal cortices and with t-tau in medial prefrontal regions. Within AD, Mini-Mental State Examination scores were associated with [^{18}F]AV1451-PET, but not CSF biomarkers.

Conclusion
[^{18}F]AV1451-PET and CSF p-tau had comparable value for differential diagnosis. Correlations were robust in a heterogeneous clinical group but attenuated (although significant) in AD, suggesting that fluid and imaging biomarkers capture different aspects of tau pathology.

Classification of evidence
This study provides Class III evidence that, in a clinical sample of patients with a variety of suspected neurodegenerative diseases, both CSF p-tau and [^{18}F]AV1451 distinguish AD from non-AD conditions.

MORE ONLINE

→ **Class of Evidence**
Criteria for rating therapeutic and diagnostic studies
NPub.org/coe

From the Memory and Aging Center (R.L.J., A.B., N.A., V.B., A.L.B., J.C., A.K., A.M., Z.A.M., J.P., H.J.R., R.T., A.V., B.L.M., G.D.R.), University of California San Francisco; Knight Alzheimer's Disease Research Center (A.M.F., G.J.), Department of Neurology (A.M.F., G.J.), and The Hope Center for Neurological Disorders (A.M.F., G.J.), Washington University in St. Louis, MO; Molecular Biophysics and Integrated Bioimaging Division (S.L.B., J.P.O., W.J.J.), Lawrence Berkeley National Laboratory, Berkeley, CA; and Helen Wills Neuroscience Institute (A.M., W.J.J., G.D.R.), University of California Berkeley.

Go to Neurology.org/N for full disclosures. Funding information and disclosures deemed relevant by the authors, if any, are provided at the end of the article.

Glossary

Aβ = β-amyloid; **AD** = Alzheimer disease; **AUC** = area under the curve; **CI** = confidence interval; **GM** = gray matter; **LBNL** = Lawrence Berkeley National Laboratory; **MCI** = mild cognitive impairment; **MMSE** = Mini-Mental State Examination; **p-tau** = phosphorylated tau; **PHF-tau** = paired helical filaments of tau; **PiB** = Pittsburgh compound B; **ROC** = receiver operating characteristic; **SPM12** = Statistical Parametric Mapping 12; **SUVR** = standard uptake value ratio; **t-tau** = total tau; **UCSF** = University of California San Francisco.

Imaging and CSF-based biomarkers both capture key aspects of Alzheimer disease (AD) pathophysiology, including β-amyloid (Aβ) and tau deposition and neurodegeneration. The applications of biomarkers in clinical and research criteria[1,2] have been predicated on the notion that imaging and CSF biomarkers can be used interchangeably to detect these pathophysiologic processes in individual patients.[3] Indeed, previous studies have demonstrated good agreement between CSF $A\beta_{42}$ and Aβ-specific PET ligands in classifying individuals as Aβ-positive or Aβ-negative.[4,5]

CSF measures of phosphorylated tau (p-tau) have been linked to neurofibrillary pathology, whereas CSF total tau (t-tau) is thought to represent a less specific marker of neurodegeneration.[3] [^{18}F]AV1451 is a novel PET radiotracer[6–8] that binds to the paired helical filaments of tau (PHF-tau) that comprise neurofibrillary tangles.[9,10] Early studies assessing the relationship between [^{18}F]AV1451-PET and CSF tau measures have reported weak to moderate relationships at the preclinical and predementia stages of AD.[11,12] Further work in more clinically relevant samples is needed to determine if imaging and fluid biomarkers provide similar information in detecting and quantifying PHF-tau pathology in vivo.

In the present study, we assessed CSF [^{18}F]AV1451-PET relationships in a heterogeneous clinical sample that consisted of patients in more advanced clinical stages of AD (primarily mild dementia) and those with non-AD dementias. We hypothesized that [^{18}F]AV1451 would best correlate with CSF p-tau compared to CSF $A\beta_{42}$ and t-tau, and that both [^{18}F]AV1451-PET and CSF p-tau would distinguish AD from non-AD dementias with high accuracy.

Methods

Patients

This retrospective study included 53 patients who were recruited from the University of California San Francisco (UCSF) Memory and Aging Center beginning in September 2013 and had available CSF and [^{18}F]AV1451-PET data by February 2017. All patients received a comprehensive clinical evaluation.[8] Clinical diagnosis was established by consensus in a multidisciplinary conference blinded to CSF and PET results. Twenty-five patients were diagnosed with probable AD dementia[1] and 3 patients with mild cognitive impairment (MCI) due to AD.[13] Remaining patients had a clinical diagnosis of a non-AD neurodegenerative disease: progressive supranuclear palsy[14] (n = 7), nonfluent primary progressive aphasia[15] (n = 6), corticobasal syndrome[16] (n = 5), behavioral variant frontotemporal dementia[17] (n = 4) or MCI not due to AD[13] (n = 3).

Patient classification was later refined based on Aβ-PET results (see below and figure 1). Among the 28 patients with a clinical diagnosis of AD, 24 were Aβ-PET-positive (23 using [^{11}C] Pittsburgh compound B [PiB], 1 using ^{18}F-florbetapir) and were included in the Aβ-positive AD group. The remaining patients, including the 25 patients with non-AD diagnoses (4 with a visual positive PiB-PET, 20 PiB-PET-negative, 1 missing data) and the 4 patients with clinical AD but a PiB-PET-negative scan, were included in the non-AD conditions group.

Standard protocol approvals, registrations, and patient consents

Written informed consent was obtained from all patients or their surrogates. The study was approved by the University of California (San Francisco and Berkeley) and Lawrence Berkeley National Laboratory (LBNL) institutional review boards for human research.

Lumbar puncture

Collection and processing of CSF samples followed Alzheimer's Disease Neuroimaging Initiative protocols (adni.loni.usc.edu/wp-content/uploads/2008/07/adni2-procedures-manual.pdf). CSF was obtained by lumbar puncture using a 25-G needle and collected in 10-mL polypropylene tubes (Sarstedt; Nümbrecht, Germany). Within 1 hour, CSF was centrifuged at 2,000*g* for 10 minutes at 4°C, transferred to new polypropylene tubes, and stored at −80°C until biomarker analysis. Analyses were performed at Washington University using INNO-BIA AlzBio3 (Innogenetics; Ghent, Belgium) assay to measure $A\beta_{42}$, p-tau 181, and t-tau, blind to clinical or imaging information.

Imaging

Acquisition

Acquisition procedures are fully described in appendix e-1 (links.lww.com/WNL/A70). Briefly, a T1-weighted sequence

Figure 1 Flowchart of patient selection and grouping

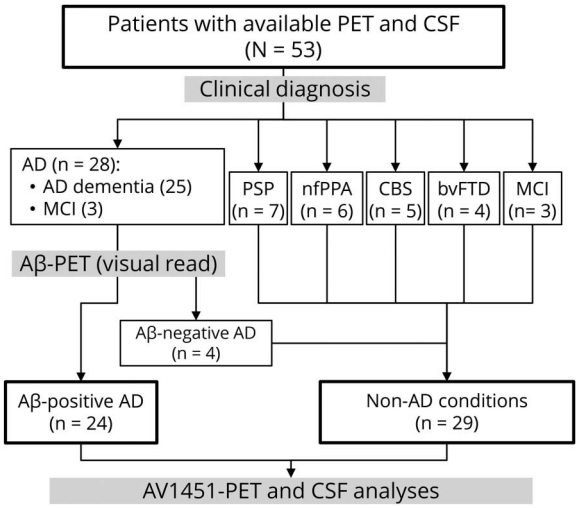

Aβ = β-amyloid; AD = Alzheimer disease; bvFTD = behavioral variant of frontotemporal dementia; CBS = corticobasal syndrome; MCI = mild cognitive impairment; nfPPA = nonfluent variant of primary progressive aphasia; PSP = progressive supranuclear palsy.

was acquired on a 3T Siemens (Munich, Germany) scanner at UCSF while PET scans were performed at LBNL on a Siemens Biograph PET/CT scanner. We analyzed data acquired from 50 to 70 minutes postinjection for ^{11}C-PiB, and 80–100 minutes postinjection for [^{18}F]AV1451.

Preprocessing

Images were processed blind to CSF results (see appendix e-2 for details, links.lww.com/WNL/A70). T1 MRIs were segmented using Freesurfer[18] version 5.3 (surfer.nmr.mgh.harvard.edu), and warped with Statistical Parametric Mapping 12 (SPM12; Wellcome Department of Imaging Neuroscience, Institute of Neurology, London, UK). PET images were coregistered onto their corresponding MRI and standard uptake value ratios (SUVRs) were created using tracer-specific reference regions: cerebellar gray matter (GM) for PiB, inferior cerebellar GM for [^{18}F]AV1451.[19] [^{18}F]AV1451 SUVR maps were then warped to template space. PET data were not corrected for partial volume effects.

Measures of interest

^{11}C-PiB scans were visually read as positive or negative by an expert neurologist (G.D.R.) as previously described[20] and global cortical ^{11}C-PiB SUVR values were extracted in native space using a large Freesurfer-defined cortical region of interest.[21]

Two complementary global metrics were extracted from [^{18}F]AV1451 (see appendix e-2 for detailed description, links.lww.com/WNL/A70). First, a mean cortical SUVR was extracted in native space using all Freesurfer-derived cortical regions as an indicator of tau cortical burden. Second, we calculated an index of spatial extent by measuring the percent of GM voxels that had significant elevated [^{18}F]AV1451 binding, as an indicator of the spread of tau pathology. This was done by comparing each patient's warped SUVR image to an independent group of 53 PiB-negative cognitively normal individuals using a W-score procedure adjusting for age.[22,23] Abnormal voxels were defined as those with W > 2 (corresponding to the 97.7th percentile of a normal distribution), but results were identical when using W > 1.65 (95th percentile) or 3 (99.9th percentile). Note that control individuals did not have CSF data and were solely included to compute W-score maps.

Statistical analyses

Our first objective was to assess the ability of [^{18}F]AV1451 and CSF measures to distinguish between patients with AD vs non-AD conditions. Biomarker values were compared between the Aβ-positive AD and non-AD conditions groups using Mann-Whitney tests. Receiver operating characteristic (ROC) analyses were conducted to assess each variable's ability to discriminate the groups; the area under the curve (AUC) and exact binomial 95% confidence intervals (95% CI) were computed. Optimal thresholds were determined using the Youden index. This evidence derived from this study is rated Class III because of the diagnostic case–control design and the risk of spectrum bias (there was little diagnostic uncertainty between the AD cases and non-AD controls). In addition, the patients were included based on the availability of both CSF and [^{18}F]AV1451-PET data.

Second, associations between [^{18}F]AV1451-PET and CSF measures were assessed using skipped Pearson correlation coefficients[24]; significance was determined using bootstrap 95% CIs to limit the influence of outliers and data heteroscedasticity. Correlations were assessed twice for each pair of variables: in the full group (n = 53), and in the Aβ-positive AD group (n = 24).

Equivalent analyses were conducted voxelwise using SPM12 2-sample *t*-test and independent multiple regression routines to perform group comparisons and PET–CSF associations. All results were displayed using a $p_{\text{uncorrected}} < 0.005$ at the voxel level combined with a $p_{\text{FWE-corrected}} < 0.05$ at the cluster level. To simplify the interpretation of voxelwise results, T-maps were transformed to effect size maps (for group comparisons) or correlation coefficient maps (for PET–CSF associations). To mirror the analyses conducted on numerical variables, ROC analyses were run to compare the 2 groups using the Voxelstats toolbox,[25] enabling the computation of AUC values voxelwise.

Third, we conducted analyses on the association between fluid and imaging biomarkers for the other 2 pathologic features of AD: Aβ and neurodegeneration.[3] We assessed correlations between (1) CSF $A\beta_{42}$ levels and cortical PiB SUVR values and (2) CSF t-tau levels and GM volumes in a voxelwise SPM12 analysis controlling for intracranial volume.

Table Group demographics

	Aβ-PET-positive AD (n = 24)	Non-AD conditions (n = 29)	Group comparison, *p* value
Age, y	61.5 ± 8.6	65.6 ± 9.1	0.10
Education, y	16.9 ± 2.8	16.5 ± 4.3	0.70
Female, n (%)	14 (58)	14 (48)	0.58
MMSE	21.5 ± 5.7	24.4 ± 6.1	0.09
CDR (0, 0.5, 1, 2), n	1, 9, 13, 1	4, 20, 3, 2	0.006
Months between CSF and [^{18}F]AV1451	5.1 ± 7.6	5.0 ± 7.3	0.98

Abbreviations: Aβ = β-amyloid; AD = Alzheimer disease; CDR = Clinical Dementia Rating; MMSE = Mini-Mental State Examination.
Values represent mean ± SD for continuous variables and actual numbers for categorical and discrete variables. Groups were compared using *t* tests for continuous variables, Fisher exact test for sex, and Mann-Whitney test for CDR.

Results

Group comparison

Patient demographics are shown in the table. Groups were matched for sex, education, and PET–CSF time difference, but the Aβ-positive AD group tended to be slightly younger and more impaired than the non-AD conditions group.

Voxelwise [^{18}F]AV1451 comparisons showed increased binding in most of the cortex in patients with Aβ-positive AD vs non-AD conditions (figure 2). This difference was maximal in temporoparietal cortices, where effect sizes reached 3 and AUC values exceeded 0.95. The 2 groups strongly differed on all biomarkers (figure 2), with Mann-Whitney *Z* values between 3.75 and 5.41 (all *p*s < 0.001) and AUC ≥ 0.80. Note that group differences were maximal for [^{18}F]AV1451-derived measures and CSF p-tau ($Z > 5$, AUC > 0.9), whereas CSF $A\beta_{42}$ and t-tau showed greater between-group overlap.

Associations between [^{18}F]AV1451-PET and CSF biomarkers

Global [^{18}F]AV1451-PET metrics vs CSF

Correlations between global [^{18}F]AV1451 metrics and CSF biomarkers are shown in figure 3. Although the statistical distribution of values differed between [^{18}F]AV1451 cortical SUVR and spatial extent, the former showing a uniform distribution while the latter follows a more bimodal pattern that splits between the AD and non-AD groups, the patterns of correlations with CSF biomarkers were comparable.

In the full sample, all CSF biomarkers significantly correlated with [^{18}F]AV1451 indices (all $|r|$s > 0.49, with negative values for CSF $A\beta_{42}$ and positive values for p-tau and t-tau), with maximal correlations ($r = 0.75$) found for CSF p-tau. As all 3 CSF biomarkers were correlated (see figure e-1, links.lww.com/WNL/A69), they were included in a robust (bisquare) regression model to distinguish individual biomarker contributions in a combined model to predict [^{18}F]AV1451 cortical SUVR. The full model explained 66.7% of total variance (adj$R^2 = 0.647$), and CSF $A\beta_{42}$ and CSF p-tau but not CSF t-tau were significant predictors (standardized estimates ± SE: $A\beta_{42}$: −0.257 ± 0.084, $p = 0.004$; p-tau: 0.561 ± 0.130, $p < 0.001$; t-tau: 0.161 ± 0.127, $p = 0.21$). Results were comparable when predicting [^{18}F]AV1451 spatial extent.

When restricted to the Aβ-positive AD group, [^{18}F]AV1451 measures were not significantly correlated with CSF $A\beta_{42}$ ($|r| < 0.05$) and were only modestly correlated with CSF t-tau and p-tau (*r*s between 0.36 and 0.51, most being statistically significant at $p < 0.05$, figure 3).

Associations between tau biomarkers and disease severity

We tested for associations between tau biomarkers and Mini-Mental State Examination (MMSE) scores in the Aβ-positive AD group. Correlations with CSF biomarkers were weak and not statistically significant: p-tau $r = 0.13$ (−0.28, 0.49); t-tau $r = -0.02$ (−0.50, 0.46). In contrast, lower MMSE was associated with greater [^{18}F]AV1451 spatial extent ($r = -0.40$ [−0.62, −0.10]) and [^{18}F]AV1451 cortical SUVR ($r = -0.31$ [−0.64, 0.05]), although the latter was not statistically significant at $\alpha = 0.05$.

Voxelwise associations

When conducted in the full sample, voxelwise associations were significant for all CSF biomarkers (figure 4). Lower CSF $A\beta_{42}$ values were associated with higher [^{18}F]AV1451 in temporoparietal areas (with *r* values reaching −0.55). CSF p-tau showed a stronger correlation, with higher p-tau being associated with higher [^{18}F]AV1451 SUVR (reaching $r = 0.8$ in the temporoparietal and dorsal frontal areas). Higher CSF t-tau values were associated with higher [^{18}F]AV1451 SUVR, although the topography of the correlations differed, peaking in the medial prefrontal lobes (reaching $r = 0.75$).

When restricted to the Aβ-positive AD group, CSF $A\beta_{42}$ was no longer associated with [^{18}F]AV1451 (figure 4). CSF p-tau and t-tau showed voxelwise associations that were comparable, but less extensive than in the full sample analyses, with a dorsal-posterior pattern for the former contrasting with a ventral-anterior pattern for the latter. The reduction in statistical significance was not only due to a decrease in statistical power (going from n = 53 to n = 24), but also to a drop in *r* values (see histograms in figure 4).

Fluid vs imaging classification as tau-positive: Performance and outliers

Using the thresholds derived from our ROC analyses (see above) to classify patients as tau-positive or tau-negative, CSF p-tau and [^{18}F]AV1451 (cortical SUVR or spatial extent) agreed in 87% of cases (Cohen κ = 0.738 [0.560, 0.961]), while CSF t-tau and [^{18}F]AV1451 had an 85% agreement rate (κ = 0.683 [0.487, 0.879]). Using previously published CSF thresholds,[26] agreement was 83% for CSF p-tau and [^{18}F]

Figure 2 Group comparisons on [^{18}F]AV1451-PET and CSF biomarkers

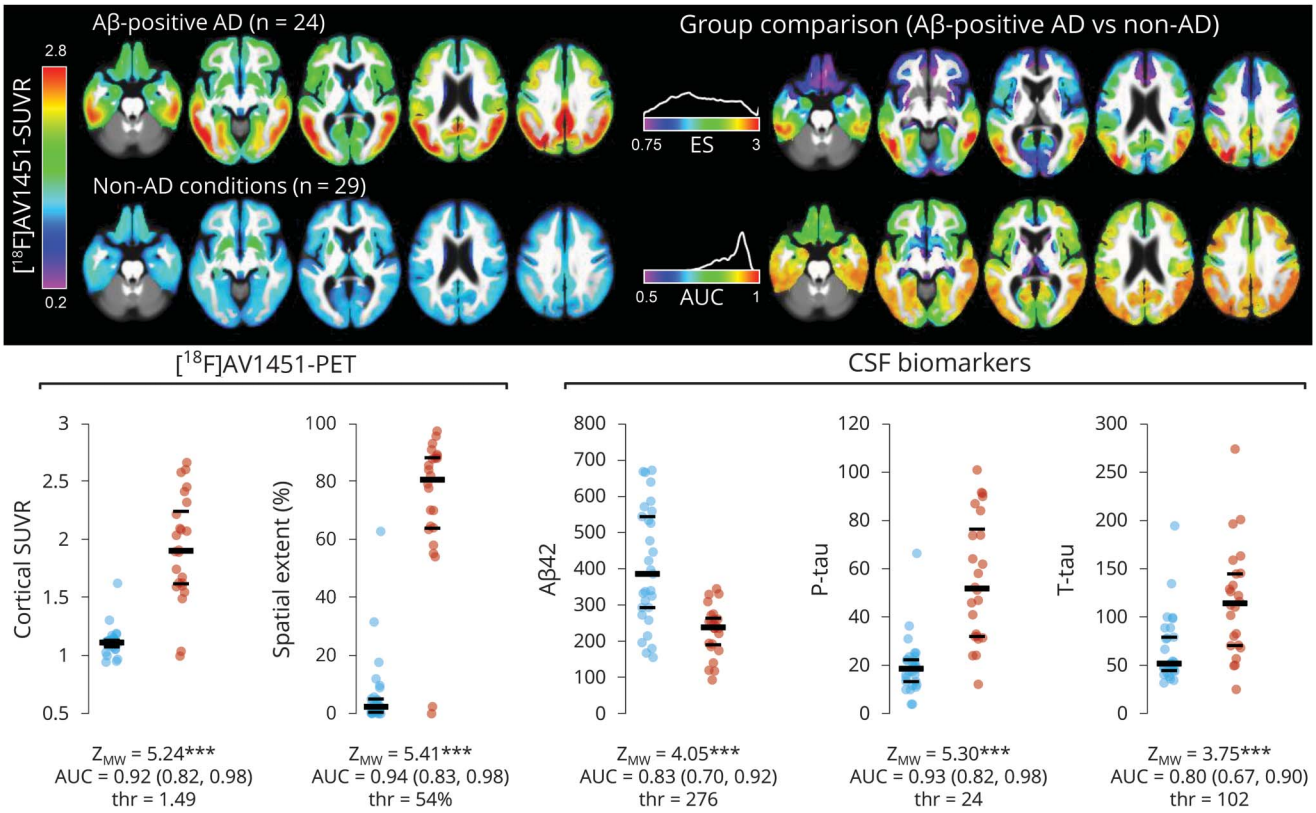

Top panel shows average patterns of [^{18}F]AV1451–standard uptake value ratio (SUVR) in the gray matter (GM) in each clinical group (left), as well as the group comparison (thresholded combining $p_{uncorrected} < 0.005$ at the voxel level and $p_{FWE\text{-}corrected} < 0.05$ at the cluster level) expressed as effect size (ES). Voxelwise receiver operating characteristic (ROC) curve analysis was also performed and the area under the curve (AUC) map is shown. The histograms of ES and AUC values within the GM mask are indicated above each corresponding colorbar. Bottom panel shows group comparison on global [^{18}F]AV1451 indices as well as CSF biomarkers. Scatterplots show individual patient values (red: β-amyloid [Aβ]–positive Alzheimer Disease [AD], blue: non-AD conditions) as well as the 1st, 2nd, and 3rd quartiles (black lines). Groups were compared using Mann-Whitney test (corresponding Z value is indicated; ***$p < 0.001$), and a ROC analysis was run to obtain AUC value (with binomial exact 95% confidence interval) and optimal threshold according to the Youden index. p-tau = Phosphorylated tau; t-tau = total tau.

AV1451 (κ = 0.666 [0.474, 0.858]) and 79% for CSF t-tau and [^{18}F]AV1451 (κ = 0.571 [0.348, 0.794]).

Four patients appeared as interesting outliers (see figure e-2 for details, links.lww.com/WNL/A69). Three patients from the Aβ-positive AD group showed discrepant tau biomarkers (the other 21 being positive on CSF p-tau and [^{18}F]AV1451): 2 patients had negative [^{18}F]AV1451-PET although CSF p-tau was (slightly) positive, while one patient had a negative CSF p-tau but a clearly positive [^{18}F]AV1451-PET. Finally, one patient from the non-AD group had [^{18}F]AV1451-PET and CSF values in the range of the Aβ-positive AD group (figure 3). Further investigations showed that this patient had a false-negative PiB-PET read.

Fluid/imaging associations for amyloid and neurodegeneration

Relationships between cortical ^{11}C-PiB-PET SUVR and CSF $A\beta_{42}$ are illustrated in figure e-3 (links.lww.com/WNL/A69). Significant correlations were found between both Aβ biomarkers when considering the full sample (r = −0.60 [−0.74, −0.44]), but not when the analysis was restricted to the 23 PiB-positive patients with AD (r = 0.13 [−0.32, 0.51]).

Regarding neurodegeneration biomarkers, voxelwise analyses showed that higher CSF t-tau was mildly associated with lower right parietal volumes (reaching r = −0.50) when all patients were included, while no relationship remained significant when restricting the analysis to the Aβ-positive AD group (figure e-3, links.lww.com/WNL/A69).

Discussion

In this study, we sought to examine relationships between [^{18}F]AV1451-PET and CSF-based tau measures in a heterogeneous group of patients, in order to compare their ability (1) to differentiate AD vs non-AD causes of cognitive impairment and (2) to quantify the severity of tau pathology in AD. Overall, measures derived from [^{18}F]AV1451-PET were strongly related to CSF biomarkers, and especially to measurements of p-tau (r = 0.75). Indeed, when used to classify patients as tau-positive, CSF p-tau and [^{18}F]AV1451 metrics performed comparatively in ROC analyses and reached

Figure 3 Correlations between global [^{18}F]AV1451-PET indices and CSF biomarkers

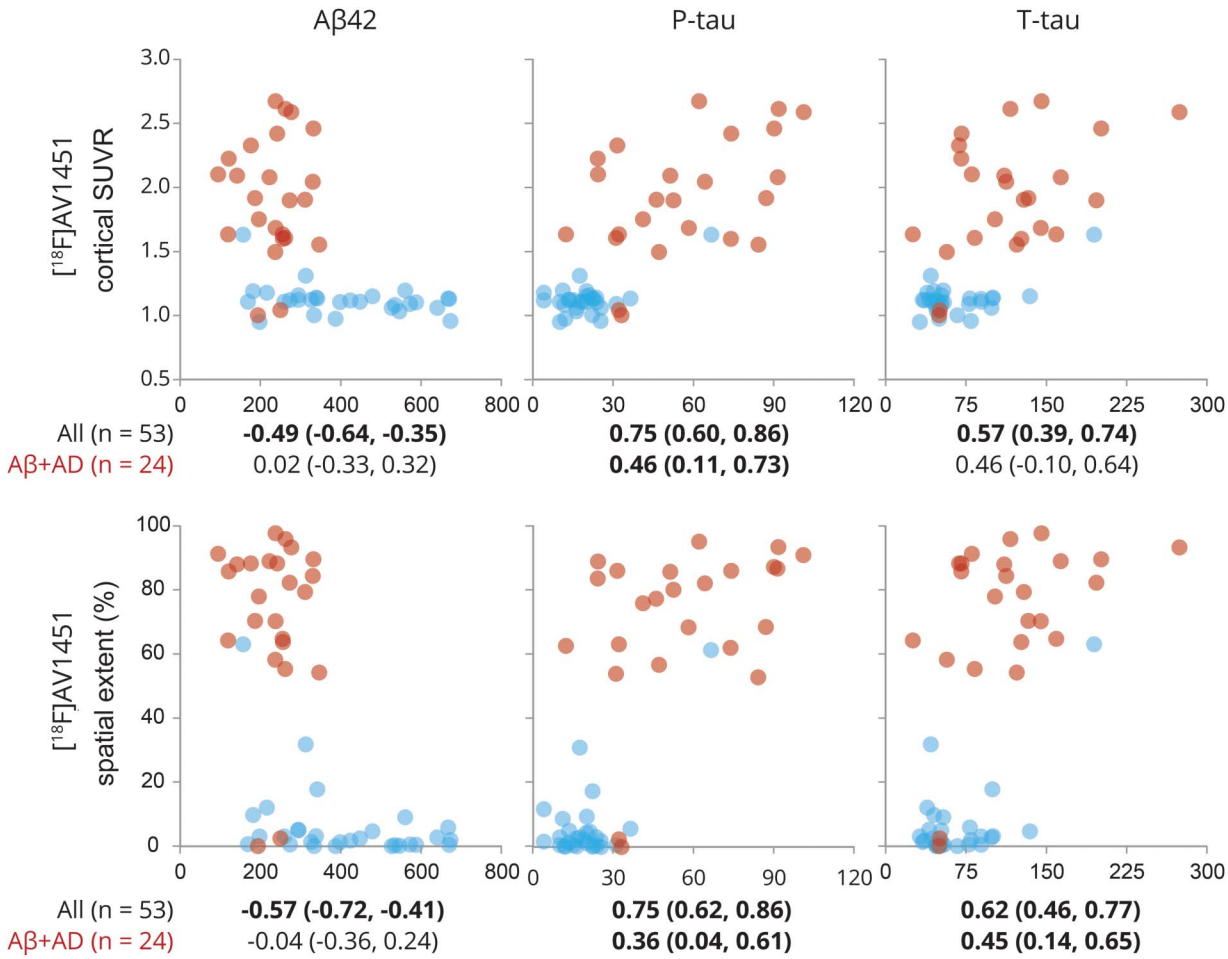

For each pair of variables, skipped correlation coefficients and corresponding bootstrap 95% confidence intervals (CI) were calculated for the full patient group and for the β-amyloid (Aβ)–positive Alzheimer disease (AD) group only; significant correlations (i.e., when 95% CI does not include 0) are bolded. Red = Aβ-positive AD; blue = non-AD conditions. p-tau = Phosphorylated tau; SUVR = standard uptake value ratio; t-tau = total tau.

satisfying agreement (83%–87%, κ = 0.67–0.74). However, quantitative correlations between [^{18}F]AV1451 and CSF p-tau were only modest when assessed within AD.

The close relationship between [^{18}F]AV1451-PET and CSF p-tau is in line with the recently proposed A/T/N (i.e., amyloid/tau/neurodegeneration) classification scheme[3] that considers tau-PET and CSF p-tau as the relevant biomarkers to classify individuals as tau-positive or tau-negative. In our cohort, the agreement between fluid and PET biomarkers of tau was in the range of what has been reported for Aβ markers.[4,27–30] In contrast, the existing literature indicates that fluid and imaging biomarkers of neurodegeneration are poorly associated (κ values are systematically below 0.4[30,31]), in line with the mild correlations we observed between CSF t-tau and GM volumes in the full group.

It is important to note that our non-AD group included patients with syndromes that are associated with a high likelihood of underlying non-AD tauopathies. For instance, 88% of patients with nonfluent primary progressive aphasia seen at our center were shown to have tau pathology at autopsy.[32] Yet both [^{18}F]AV1451 and CSF p-tau discriminated the non-AD group from Aβ-positive patients with AD, highlighting that both these biomarkers are more strongly linked to PHF-tau than to other forms of tauopathy. Our results are consistent with previous reports on the specificity of CSF p-tau,[33] and with postmortem and in vivo studies indicating a higher affinity of [^{18}F]AV1451 for PHF-tau compared to other tauopathies.[9,10]

In contrast with the high CSF/PET associations observed in the full group, correlations were mild when restricted to the Aβ-positive AD group, dropping to below $r = 0.5$ for global indices of [^{18}F]AV1451-PET (i.e., less than 25% of shared variance), similar to previously reported correlations in cognitively normal older adults.[11] This pattern was even more pronounced for biomarkers of Aβ and neurodegeneration, as

Figure 4 Voxelwise associations between [^{18}F]AV1451 and CSF biomarkers

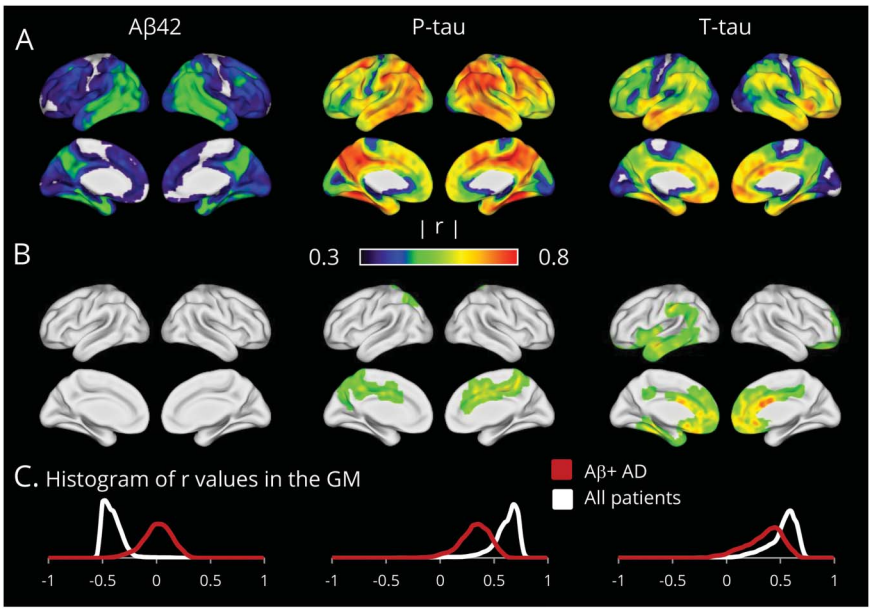

Results are shown using a threshold combining $p_{uncorrected} < 0.005$ at the voxel level and $p_{FWE\text{-}corrected} < 0.05$ at the cluster level, and T-values were converted to *r* values for illustration purposes. The associations were assessed in the full group (A) and the β-amyloid (Aβ)–PET-positive Alzheimer disease (AD) group only (B). Row C illustrates the distribution of *r* values in the entire gray matter (GM) mask when assessing the full group (white) and the Aβ-positive AD group only (red). For simplicity, the colorscale used on the 3D renders shows the absolute values of *r* but correlation coefficients were strictly negative for CSF $A\beta_{42}$ and strictly positive for all other biomarkers, as shown on the histograms. p-tau = Phosphorylated tau; t-tau = total tau.

correlations between fluid and imaging markers were significant at the whole group level, but not within the Aβ-positive AD group. Yet, inspection of scatterplots (figure 3) shows that both CSF p-tau and [^{18}F]AV1451-PET measures have a broad dynamic range, arguing against a simple ceiling effect and suggesting that fluid and imaging markers might capture different aspects of tau biology.

Interestingly, and although this is still debated,[34] accumulating evidence suggests that CSF p-tau may increase in an early disease stage and later decrease in symptomatic patients with AD.[35–37] It has therefore been hypothesized that early p-tau increases reflect the progression of tau pathology throughout the brain (i.e., when the size of neuronal populations developing tau pathology increases)[36] while p-tau would later decrease due to the death of neurons. Alternatively, p-tau might become sequestrated in tangles. CSF p-tau levels would therefore be expected to vary nonlinearly by disease stage whereas [^{18}F]AV1451-PET signal might reflect the overall accumulation of pathology. This is supported by the current data showing that lower MMSE was correlated with increased [^{18}F]AV1451-PET binding, but not CSF p-tau in the AD group. Assessing longitudinal changes in both p-tau and [^{18}F]AV1451-PET is necessary to determine the specific dynamics of each marker.

It should be noted that patterns of correlations and diagnostic properties were highly similar using [^{18}F]AV1451 cortical SUVR and spatial extent, in spite of the different statistical distributions of these global measures. Voxelwise analyses suggest that a more regional approach targeting specific regions (e.g., precuneus) might help strengthen the correlations between p-tau and tau-PET within the AD group.

Comparison of the correlation patterns observed between [^{18}F]AV1451 PET and CSF p-tau vs CSF t-tau revealed an interesting pattern, in spite of the strong intercorrelation of these 2 biomarkers. At the full group level, [^{18}F]AV1451 was more strongly correlated with CSF p-tau than CSF t-tau, consistent with the idea that p-tau is a better marker of PHF tau pathology than t-tau.[3] However, this hierarchy disappeared when restricting the analyses to the Aβ-positive AD group. Moreover, the voxelwise regression analyses showed a differential pattern of regional correlation, with CSF p-tau correlating with temporoparietal [^{18}F]AV1451 (the areas of highest and most frequent uptake in AD) while CSF t-tau was associated with [^{18}F]AV1451 in prefrontal cortex, an area affected by tau in later stages of AD.[38] Given the modest size of our Aβ-positive AD group, we consider this finding preliminary. However, if replicated in larger samples, this finding could indicate that elevated t-tau is a marker of more advanced disease stage as defined by more widespread tau pathology and neurodegeneration.

Our study has limitations. The sample size was modest (though comparable to previous tau-PET vs CSF studies). Our patients on average represented an early age at onset dementia cohort, in which contrasts in CSF and PET measures of tau may be heightened in AD vs non-AD conditions compared to older cohorts. CSF data were only available in symptomatic patients while data from cognitively normal controls would provide data on earlier stages of tau pathology, allowing better characterization of CSF

imaging relationships across the AD continuum. Finally, the cross-sectional nature of our study does not allow us to clearly determine the actual ordering and evolution of biomarker abnormalities over time.

Overall, the present data support the notion that CSF p-tau and [^{18}F]AV1451-PET uptake are reliable biomarkers to detect PHF-tau in a clinical sample. Further research is needed to assess longitudinal changes in both fluid and imaging biomarkers, which will be crucial to model disease progression and evaluate upcoming anti-tau therapeutics.[39]

Author contributions

Renaud La Joie: study concept and design, drafting/revising the manuscript for content, analysis and interpretation of data, statistical analysis. Alexandre Bejanin: revising the manuscript for content, contribution of vital tools. Anne M. Fagan: drafting/revising the manuscript for content, analysis and interpretation of data. Nagehan Ayakta: data acquisition and analysis. Suzanne L. Baker: revising the manuscript for content, contribution of vital tools. Viktoriya Bourakova: analysis of data, revising the manuscript. Adam L. Boxer: study concept, obtaining funding. Jungho Cha: revising the manuscript for content, contribution of vital tools. Anna Karydas: data analysis, contribution of vital tools. Gina Jerome: data analysis, contribution of vital tools. Anne Maass: revising the manuscript for content, contribution of vital tools. Ashley Mensing: data acquisition and analysis. Zachary A. Miller: study concept, obtaining funding. James P. O'Neil: analysis of data, revising the manuscript. Julie Pham: data acquisition and analysis. Howard J. Rosen: study concept, obtaining funding. Richard Tsai: study concept, data acquisition. Adrienne V. Visani: analysis of data, revising the manuscript. Bruce L. Miller: study concept, obtaining funding. William J. Jagust: revising the manuscript for content, obtaining funding. Gil D. Rabinovici: study concept and design, drafting/revising the manuscript for content, study supervision, obtaining funding.

Acknowledgment

The authors thank the study participants and their families for their contribution to research.

Study funding

Supported by the Alzheimer's Association (AARF-16-443577 to R.L.J.), Tau Consortium (to G.D.R. and W.J.J.), National Institute on Aging grants (R01-AG045611 to G.D.R., R01-AG034570 to W.J.J., P50-AG023501 to B.L.M. and G.D.R., P01-AG19724 to W.J.J. and B.L.M., 4TNIR01-AG038791 to A.L.B., G.D.R., and W.J.J., ARTFL U54-NS092089 to A.L.B., B.L.M., G.D.R., and H.J.R.), State of California Department of Health Services Alzheimer's Disease Research Centre of California grant (04–33516 to B.L.M.), and Michael J. Fox Foundation (to G.D.R. and W.J.J.). Avid Radiopharmaceuticals enabled use of the [^{18}F]AV1451 tracer by providing precursor, but did not provide direct funding and was not involved in data analysis or interpretation.

Disclosure

R. La Joie and A. Bejanin report no disclosures relevant to the manuscript. A. Fagan is supported by NIH grants including P50AG005681, P01AG003991, P01AG026276, and UF01AG03243807. Dr. Fagan is on the Scientific Advisory Boards for Roche Diagnostics, IBL International, and AbbVie and consults for Biogen, DiamiR LLC, LabCorp, and Araclon Biotech/Griffols. N. Ayakta, S. Baker, and V. Bourakova report no disclosures relevant to the manuscript. A. Boxer receives research support from Avid, Biogen, Bristol Myers Squibb, C2N Diagnostics, Cortice Biosciences, Eli Lilly, Forum Pharmaceuticals, Genentech, and TauRx. He has served as a consultant for Asceneuron, Ipierian, Isis, Janssen, and Merck. He has stock/options in Alector and Delos. J. Cha, A. Karydas, G. Jerome, A. Maass, and A. Mensing report no disclosures relevant to the manuscript. Z. Miller is funded by an NIH grant (K23 AG048291). J. O'Neil receives research support from Genzyme Corp, the US Department of Energy, the US Army Medical Research & Materiel Command, and the NIH. J. Pham reports no disclosures relevant to the manuscript. H. Rosen receives research support from NIH/National Institute on Aging, RO1 AG032306 (PI), PO1 AG019724 (Core leader), AG045333 (PI), and AG023501 (core leader). R. Tsai receives research support from the University of California. He also consulted for ExpertConnect and Grifols. A. Visani reports no disclosures relevant to the manuscript. B. Miller receives grant support from the NIH/NIA and the Centers for Medicare & Medicaid Services as grants for the Memory and Aging Center. As an additional disclosure, Dr. Miller serves as Medical Director for the John Douglas French Foundation; Scientific Director for the Tau Consortium; Director/Medical Advisory Board of the Larry L. Hillblom Foundation; Scientific Advisory Board Member for the National Institute for Health Research Cambridge Biomedical Research Centre and its subunit, the Biomedical Research Unit in Dementia (UK); and Board Member for the American Brain Foundation (ABF). W. Jagust has served as a consultant to BioClinica, Genentech, and Novartis Pharmaceuticals. G. Rabinovici receives research support from Avid Radiopharmaceuticals, GE Healthcare, and Piramal, and has received consulting fees or speaking honoraria from Roche, Eisai, Lundbeck, Piramal, Genentech, Merck, and Putnam. Go to Neurology.org/N for full disclosures.

Received June 15, 2017. Accepted in final form October 4, 2017.

References

1. McKhann GM, Knopman DS, Chertkow H, et al. The diagnosis of dementia due to Alzheimer's disease: recommendations from the National Institute on Aging-Alzheimer's Association workgroups on diagnostic guidelines for Alzheimer's disease. Alzheimers Dement 2011;7:263–269.
2. Dubois B, Feldman HH, Jacova C, et al. Advancing research diagnostic criteria for Alzheimer's disease: the IWG-2 criteria. Lancet Neurol 2014;13:614–629.
3. Jack CR, Bennett DA, Blennow K, et al. A/T/N: an unbiased descriptive classification scheme for Alzheimer disease biomarkers. Neurology 2016;87:539–547.
4. Blennow K, Mattsson N, Schöll M, Hansson O, Zetterberg H. Amyloid biomarkers in Alzheimer's disease. Trends Pharmacol Sci 2015;36:297–309.
5. Fagan AM, Mintun MA, Mach RH, et al. Inverse relation between in vivo amyloid imaging load and cerebrospinal fluid Abeta42 in humans. Ann Neurol 2006;59:512–519.
6. Chien DT, Bahri S, Szardenings AK, et al. Early clinical PET imaging results with the novel PHF-tau radioligand [F-18]-T807. J Alzheimers Dis 2013;34:457–468.

7. Xia C-F, Arteaga J, Chen G, et al. [(18)F]T807, a novel tau positron emission tomography imaging agent for Alzheimer's disease. Alzheimers Dement 2013;9:666–676.
8. Ossenkoppele R, Schonhaut DR, Schöll M, et al. Tau PET patterns mirror clinical and neuroanatomical variability in Alzheimer's disease. Brain 2016;139:1551–1567.
9. Lowe VJ, Curran G, Fang P, et al. An autoradiographic evaluation of AV-1451 tau PET in dementia. Acta Neuropathol Commun 2016;4:58.
10. Marquié M, Normandin MD, Vanderburg CR, et al. Validating novel tau positron emission tomography tracer [F-18]-AV-1451 (T807) on postmortem brain tissue. Ann Neurol 2015;78:787–800.
11. Chhatwal JP, Schultz AP, Marshall GA, et al. Temporal T807 binding correlates with CSF tau and phospho-tau in normal elderly. Neurology 2016;87:920–926.
12. Gordon BA, Friedrichsen K, Brier M, et al. The relationship between cerebrospinal fluid markers of Alzheimer pathology and positron emission tomography tau imaging. Brain 2016;139:2249–2260.
13. Albert MS, DeKosky ST, Dickson D, et al. The diagnosis of mild cognitive impairment due to Alzheimer's disease: recommendations from the National Institute on Aging-Alzheimer's Association workgroups on diagnostic guidelines for Alzheimer's disease. Alzheimers Dement 2011;7:270–279.
14. Litvan I, Agid Y, Calne D, et al. Clinical research criteria for the diagnosis of progressive supranuclear palsy (Steele-Richardson-Olszewski syndrome): report of the NINDS-SPSP International Workshop. Neurology 1996;47:1–9.
15. Gorno-Tempini ML, Hillis AE, Weintraub S, et al. Classification of primary progressive aphasia and its variants. Neurology 2011;76:1006–1014.
16. Armstrong MJ, Litvan I, Lang AE, et al. Criteria for the diagnosis of corticobasal degeneration. Neurology 2013;80:496–503.
17. Rascovsky K, Hodges JR, Knopman D, et al. Sensitivity of revised diagnostic criteria for the behavioural variant of frontotemporal dementia. Brain 2011;134:2456–2477.
18. Fischl B, Dale AM. Measuring the thickness of the human cerebral cortex from magnetic resonance images. Proc Natl Acad Sci USA 2000;97:11050–11055.
19. Maass A, Landau S, Baker SL, et al. Comparison of multiple tau-PET measures as biomarkers in aging and Alzheimer's disease. NeuroImage 2017;157:448–463.
20. Rabinovici GD, Rosen HJ, Alkalay A, et al. Amyloid vs FDG-PET in the differential diagnosis of AD and FTLD. Neurology 2011;77:2034–2042.
21. Villeneuve S, Rabinovici GD, Cohn-Sheehy BI, et al. Existing Pittsburgh compound-B positron emission tomography thresholds are too high: statistical and pathological evaluation. Brain 2015;138:2020–2033.
22. La Joie R, Perrotin A, Barré L, et al. Region-specific hierarchy between atrophy, hypometabolism, and β-amyloid (Aβ) load in Alzheimer's disease dementia. J Neurosci 2012;32:16265–16273.
23. Ossenkoppele R, Cohn-Sheehy BI, La Joie R, et al. Atrophy patterns in early clinical stages across distinct phenotypes of Alzheimer's disease. Hum Brain Mapp 2015;36:4421–4437.
24. Pernet CR, Wilcox R, Rousselet GA. Robust correlation analyses: false positive and power validation using a new open source MATLAB toolbox. Front Psychol 2012;3:606.
25. Mathotaarachchi S, Wang S, Shin M, et al. VoxelStats: a MATLAB package for multimodal voxel-wise brain image analysis. Front Neuroinform 2016;10:20.
26. Shaw LM, Vanderstichele H, Knapik-Czajka M, et al. Cerebrospinal fluid biomarker signature in Alzheimer's disease neuroimaging initiative subjects. Ann Neurol 2009;65:403–413.
27. Toledo JB, Bjerke M, Da X, et al. Nonlinear association between cerebrospinal fluid and florbetapir F-18 β-amyloid measures across the spectrum of Alzheimer disease. JAMA Neurol 2015;72:571–581.
28. Landau SM, Lu M, Joshi AD, et al. Comparing positron emission tomography imaging and cerebrospinal fluid measurements of β-amyloid. Ann Neurol 2013;74:826–836.
29. Zwan M, van Harten A, Ossenkoppele R, et al. Concordance between cerebrospinal fluid biomarkers and [11C]PIB PET in a memory clinic cohort. J Alzheimers Dis 2014;41:801–807.
30. Vos SJB, Gordon BA, Su Y, et al. NIA-AA staging of preclinical Alzheimer disease: discordance and concordance of CSF and imaging biomarkers. Neurobiol Aging 2016;44:1–8.
31. Alexopoulos P, Kriett L, Haller B, et al. Limited agreement between biomarkers of neuronal injury at different stages of Alzheimer's disease. Alzheimers Dement 2014;10:684–689.
32. Spinelli EG, Mandelli ML, Miller ZA, et al. Typical and atypical pathology in primary progressive aphasia variants. Ann Neurol 2017;81:430–443.
33. Tang W, Huang Q, Yao YY, Wang Y, Wu YL, Wang ZY. Does CSF p-tau181 help to discriminate Alzheimer's disease from other dementias and mild cognitive impairment? A meta-analysis of the literature. J Neural Transm 2014;121:1541–1553.
34. Toledo JB, Xie SX, Trojanowski JQ, Shaw LM. Longitudinal change in CSF Tau and Aβ biomarkers for up to 48 months in ADNI. Acta Neuropathol 2013;126:659–670.
35. Wildsmith KR, Schauer SP, Smith AM, et al. Identification of longitudinally dynamic biomarkers in Alzheimer's disease cerebrospinal fluid by targeted proteomics. Mol Neurodegener 2014;9:22.
36. Fagan AM, Xiong C, Jasielec MS, et al. Longitudinal change in CSF biomarkers in autosomal-dominant Alzheimer's disease. Sci Transl Med 2014;6:226ra30.
37. Seppälä TT, Koivisto AM, Hartikainen P, Helisalmi S, Soininen H, Herukka SK. Longitudinal changes of CSF biomarkers in Alzheimer's disease. J Alzheimers Dis 2011;25:583–594.
38. Delacourte A, David J, Sergeant N, et al. The biochemical pathway of neurofibrillary degeneration in aging and Alzheimer's disease. Neurology 1999;52:1158.
39. Mattsson N, Carrillo MC, Dean RA, et al. Revolutionizing Alzheimer's disease and clinical trials through biomarkers. Alzheimers Dement 2015;1:412–419.

SOURCE ARTICLE NPub.org/u6ydj3

Associations between [^{18}F]AV1451 tau PET and CSF measures of tau pathology in a clinical sample

Renaud La Joie, PhD, Alexandre Bejanin, PhD, Anne M. Fagan, PhD, Nagehan Ayakta, BS, Suzanne L. Baker, PhD, Viktoriya Bourakova, BA, Adam L. Boxer, MD, PhD, Jungho Cha, PhD, Anna Karydas, BS, Gina Jerome, MS, Anne Maass, PhD, Ashley Mensing, BS, Zachary A. Miller, MD, James P. O'Neil, PhD, Julie Pham, BA, Howard J. Rosen, MD, Richard Tsai, MD, Adrienne V. Visani, BS, Bruce L. Miller, MD, William J. Jagust, MD, and Gil D. Rabinovici, MD

Correspondence
Dr. La Joie
Renaud.Lajoie@ucsf.edu

Cite as: *Neurology*® 2018;90:e282-e290. doi:10.1212/WNL.0000000000004860

Study question

Can the relationships, if any, between imaging ([^{18}F]AV1451-PET) and CSF markers of tau pathology be used to differentiate between Alzheimer disease (AD)–associated and non-AD-associated cognitive impairment?

Summary answer

Both [^{18}F]AV1451-PET and CSF phosphorylated tau (p-tau) can distinguish AD from non-AD conditions, but capture different aspects of tau pathology.

What is known and what this article adds

Previous reports highlight the specificity of CSF p-tau, and postmortem and in vivo studies indicate that [^{18}F]AV1451 has a higher affinity for hyperphosphorylated tau than for other tauopathies. This study provides Class III evidence that both CSF p-tau and [^{18}F]AV1451 have the ability to differentiate AD from non-AD conditions in a clinically heterogeneous sample of patients with suspected neurodegenerative disease.

Participants and setting

Fifty-three patients were recruited from the University of California San Francisco Memory and Aging Center with available clinical diagnosis of either AD or non-AD neurodegenerative disease; 25 had probable AD dementia and 3 had AD-associated mild cognitive impairment (MCI). The remaining 25 had non-AD neurodegenerative diseases including progressive supranuclear palsy, nonfluent primary progressive aphasia, corticobasal syndrome, behavioral variant frontotemporal dementia, or non-AD MCI.

Design

Patients in this retrospective study were enrolled from September 2013 with [^{18}F]AV1451-PET and CSF data available by February 2017.

Primary outcomes

The primary outcomes were measurements of AD-related and non-AD-related neurodegeneration as well as quantification of AD tau pathology severity via imaging ([^{18}F]AV1451 PET) and CSF biomarkers.

Main results and the role of chance

Excellent discrimination as well as classification agreement (83%) was obtained via [^{18}F]AV1451-PET cortical standardized uptake value ratios and p-tau between β-amyloid (Aβ)–positive and non-AD conditions (area under the curve 0.92–0.94; ≤0.83 for other CSF measures). Cortical [^{18}F]AV1451 was associated with all CSF biomarkers and most strongly with p-tau (r = 0.75 vs 0.57 for total tau [t-tau] and −0.49 for $A\beta_{42}$) in the full sample cohort, while the correlation was strongest with p-tau and t-tau (r = 0.46 for both and 0.02 for $A\beta_{42}$) in Aβ-positive patients with AD. Voxelwise analyses revealed strong correlations between [^{18}F]AV1451 and CSF p-tau in temporoparietal cortices and t-tau in medial prefrontal regions. Mini-Mental State Examination scores were only associated with [^{18}F]AV1451 PET biomarkers for AD.

Voxelwise associations between [^{18}F]AV1451 and CSF biomarkers: (A) Analyses in the full group (n=53) and (B) analysis in the Aβ-positive AD group only (n=24)

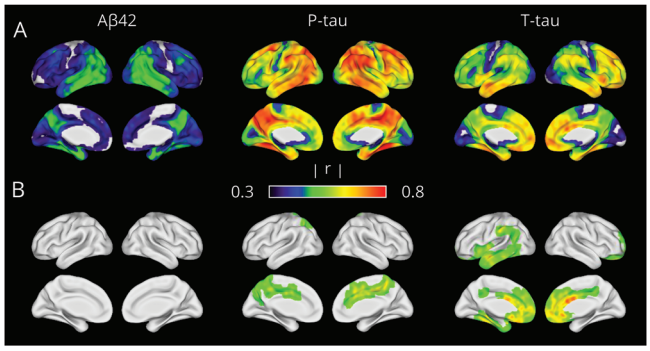

Bias, confounding, and other reasons for caution

The sample size was small, and the cohort represented patients with early-onset dementia, resulting in differing proportions of patients with AD vs without AD compared to older cohorts. CSF data were not available for controls. The cross-sectional nature of the study prevented the determination of chronological ordering and evolution of fluid and imaging biomarker abnormalities.

Generalizability to other populations

The small sample size and single recruitment site may limit generalizability.

Study funding/potential competing interests

This study was funded by the Alzheimer's Association, the Tau Consortium, several National Institute on Aging grants, the State of California Department of Health Services Alzheimer's Disease Research Center of California grant, and the Michael J. Fox foundation. Go to Neurology.org/N for full disclosures.

A draft of the short-form article was written by E. Feric, a writer with Editage, a division of Cactus Communications. The authors of the full-length article and the journal editors edited and approved the final version.